Bulletin of the Geological Society of Greece
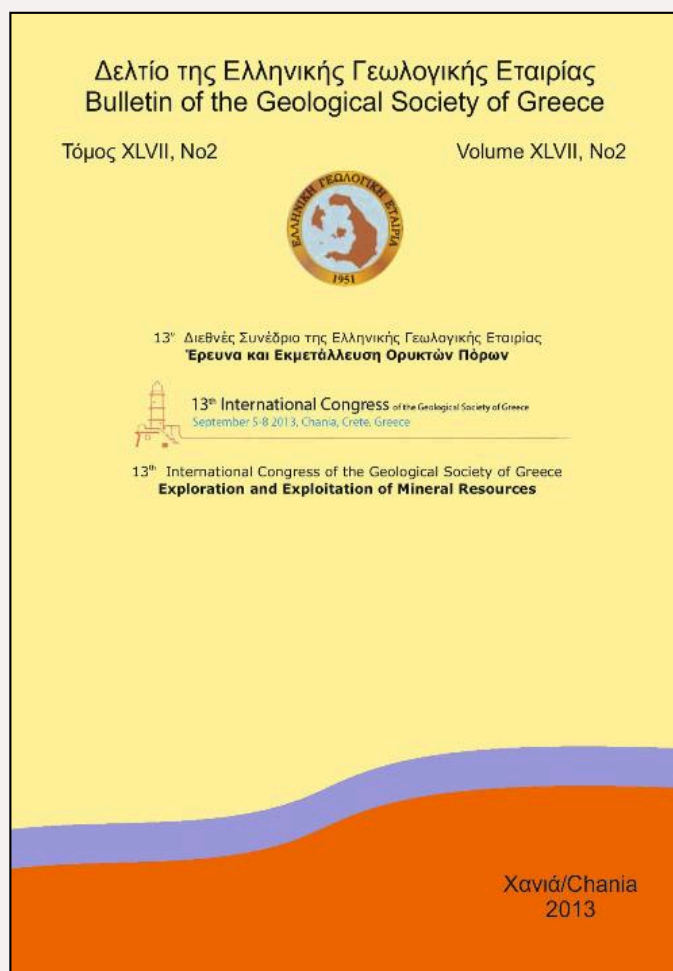
Vol. 47, 2013

Paleoearthquake history of the Spili fault

Mouslopoulou V.	Technical University of Crete, Department of Mineral Resources Engineering
Moraetis D.	Technical University of Crete, Department of Mineral Resources Engineering
Benedetti L.	Centre Européen de Recherche et d'Enseignement des Géosciences de l'Environnement (CEREGE), CNRS
Guillou V.	Centre Européen de Recherche et d'Enseignement des Géosciences de l'Environnement (CEREGE), CNRS
Hristopulos D.	Technical University of Crete, Department of Mineral Resources Engineering

To cite this article:

PALEOEARTHQUAKE HISTORY OF THE SPILI FAULT, CRETE, GREECE

Mouslopoulou V.[1], Moraetis D.[1], Benedetti L.[2], Guillou V.[2] and Hristopulos D.[1]

[1] *Technical University of Crete, Department of Mineral Resources Engineering, vasiliki@mred.tuc.gr , moraetis@mred.tuc.gr, dionisi@mred.tuc.gr*

[2] *Centre Européen de Recherche et d'Enseignement des Géosciences de l'Environnement (CEREGE), CNRS, France, benedetti@cerege.fr, guillou@cerege.fr*

Abstract

The paleoearthquake activity on the Spili Fault is examined using a novel methodology that combines measurements of Rare Earth Elements (REE) and of in situ cosmogenic ^{36}Cl on the exhumed fault scarp. Data show that the Spili Fault is active and has generated a minimum of five large-magnitude earthquakes over the last ~16500 years. The timing and, to a lesser degree, the slip-size of the identified paleoearthquakes was highly variable. Specifically, the two most recent events occurred between 100 and 900 years BP producing a cumulative displacement of 3.5 meters. The timing of the three older paleoearthquakes is constraint at 7300, 16300 and 16500 years BP with slip sizes of 2.5, 1.2 and 1.8 meters, respectively. The magnitude of the earthquakes that produced the measured co-seismic displacements, ranges from M 6.3-7.3 while the average earthquake recurrence interval on the Spili Fault is about 4200 years. The above data suggest that the Spili is among the most active faults on Crete and its earthquake parameters may be incorporated into the National Seismic Hazard Model.

Key words: *Fault, earthquake, seismic-risk.*

Περίληψη

Η παλαιοσεισμική δραστηριότητα στο ρήγμα του Σπηλίου μελετήθηκε χρησιμοποιώντας μία πρωτοποριακή μέθοδο που συνδιάζει μετρήσεις Σπανίων Γαιών (REE) και κοσμογενών ισοτόπων ^{36}Cl πάνω στην σεισμικά αποκαλυμμένη επιφάνεια του ρήγματος. Η ανάλυση των δεδομένων δείχνει ότι το ρήγμα είναι ενεργό και έχει φιλοξενήσει τουλάχιστον 5 μεγάλου-μεγέθους σεισμούς τα τελευταία 16500 χρόνια. Οι δύο πιο πρόσφατοι σεισμοί έλαβαν χώρα κατά την περίοδο 100-900 ετών πρίν από σήμερα και άθροισαν συνολικά 3.5 μέτρα σεισμικής μετατόπισης. Η χρονολογία των παλαιότερων 3 σεισμών προσδιορίσθηκε στα 7300, 16300 και 16500 χρόνια πριν από σήμερα με σεισμικές ολισθήσεις 2.5, 1.2 και 1.8 μέτρα, αντίστοιχα. Από το μέγεθος των σεισμικών ολισθήσεων συμπεραίνουμε ότι το μέγεθος των σεισμών που προκλήθηκαν από το ρήγμα του Σπηλίου κυμάνθηκε από M 6.3-7.3 ενώ ο μέσος ρυθμός επανάληψης τους ήταν ~4200 χρόνια. Τα παραπάνω δεδομένα αποκαλύπτουν ότι το ρήγμα του Σπηλίου είναι ένα από τα πιο ενεργά ρήγματα στην Κρήτη και οι

σεισμικές παράμετροί που σχετίζονται με την δραστηριότητά του πρέπει να συμπεριληφθούν στο μοντέλο σεισμικής επικινδυνότητας της Ελλάδας.
***Λέξεις κλειδιά:** Ρήγμα, σεισμός, σεισμική επικινδυνότητα.*

1. Introduction and Geological Setting

Earthquakes are one of the deadliest natural disasters. About 20% of the Earth's population lives in areas of seismic hazard. Every year, there are approximately 150 large (>6M) earthquakes worldwide, causing an average of 20,000 casualties since the beginning of the 20th century and significantly impacting the economies and the sustainable development of the affected societies. Therefore, better understanding and forecasting of earthquake occurrence is one of the most pressing humanitarian goals within the sciences. Tectonic faults are breaks in the Earth's crust that grow primarily due to large magnitude earthquakes (Stein et al., 1988). Over millions of years, large cumulative displacements (e.g. >5km) accrue on faults as a result of 100's to 1000's of earthquakes; however, the systematics of this process is poorly understood. This is mainly due to the brevity of the available instrumental and/or historic earthquake record in comparison to the repeat times of large earthquakes on most faults globally. Paleoseismological investigations (i.e. fault trenching, etc.) are capable of extending the instrumental and/or historic earthquake record by including the majority of surface rupturing prehistoric earthquakes of M>6 on any particular fault (McCalpin, 1996). The identification of the timing between, and slip during, successive earthquakes on individual faults is vital in earthquake research as it highlights, and to some extent constrains, the variability associated with the complex phenomenon of earthquake occurrence (Nicol et al., 2009). Thus, paleoseismology increases the time-window over which earthquake information is available to thousands of years, providing a more realistic estimate of the seismic hazard of a particular fault.

But how exhumed carbonate fault scarps are capable of recording past earthquakes? During a large earthquake, a portion of a normal fault plane that was previously buried is suddenly exposed to the atmosphere. As further large earthquakes occur, the exposed fault plane becomes progressively larger and the succession forms a topographic escarpment, the height of which can be attributed to a number of past earthquakes (Benedetti et al., 2002). If we could identify the sections of the scarp that became successively exposed through time, we would know the number and size of the earthquakes generated by this fault. Accordingly, if we could date those sections, then we would know the timing of each earthquake.

In the case of limestone fault scarps the number, size and timing of earthquakes may indeed be constrained. As a section of a normal fault plane is suddenly exhumed, it becomes exposed to supergene weathering (rain, wind, vegetation and bacterial activity) and cosmic radiation (secondary neutrons and muons interact with Ca of the limestone scarp). The longer the surface is exposed, the more intense the weathering and the absorption of cosmic radiation. It is known that differential weathering of limestone scarps may be recorded in the chemical content of Rare Earth Elements (REE) (Manighetti et al., 2010; Mouslopoulou et al., 2011). Specifically, the concentration of REE generally decreases up-scarp, and peaks at sections of the scarp where the limestone was in direct contact with the paleosol (the limestone becomes enriched in REE while buried below the upper soil). Thus, a fault scarp is expected to include a series of rupture zones which have been weathered and exposed to radiation over significantly different time spans. The degree of weathering will reveal the number and size of the earthquakes, whereas the cosmic radiation will constrain their timing.

The primary research objective of this study is to constrain the paleoearthquake history on the Spili Fault, a fault located on the island of Crete in Greece (Figure 1a).

The Spili Fault is a normal fault that traverses the central part of Crete with a NW-SE orientation (300-320°) (Figure 1a). It extends for ca. 20 km onshore, defining along most of its length the

boundary between the Mesozoic bedrock units of Tripoli- or Pindos-limestone (upthrown block) and Pindos-flysch or ophiolites (downthrown block) (Angelier, 1979). The dip of the Spili Fault ranges from 55° SW to 75°SW. At the localities where the paleoearthquakes were identified (sites 1 and 2), the bedrock flysch is downthrown across the fault by ca. 600 m, and an elongated northwest-trending limestone ridge is formed. At the base of the ridge, a series of alluvial fans are formed by feeder streams. The fault has vertically displaced a number of alluvial fans, exposing a 10-20 m high and steep section of its carbonate fault plane. The fault plane is brecciated and, at places, polished by repeated slip movement (Figure 1b). Several slickenside striations on the main slip surface reveal a dominantly normal sense of motion, with a minor strike-slip component (i.e. 3 10/70, 308/78, 311/80 SW) (Mouslopoulou et al., 2011).

2. Research Methodology

In order to identify the number, size and timing of the large-magnitude prehistoric earthquakes that ruptured the Spili Fault, we employed a globally novel technique that involves a) identification and measurement of the Rare Earth Elements (REE) hosted in the exhumed limestone fault scarp; b) measurement of the in situ cosmogenic ^{36}Cl on each rupture zone. The former technique will provide the number and size of the earthquakes whereas the latter, the timing of the earthquakes. Specifically, paleoearthquake investigations involved 4 individual steps:
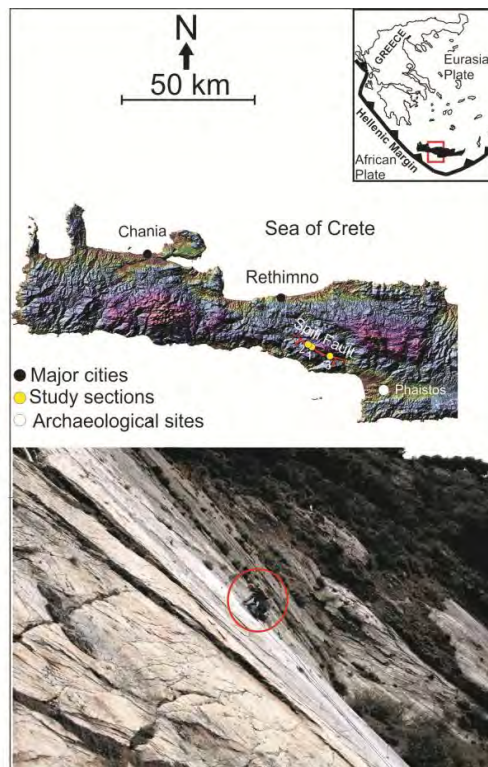

Figure 1 – Upper panel: Digital elevation model of western Crete illustrating the surface trace of the Spili Fault. The study sites are indicated by yellow circles: 1=Spili, 2=Health Center, 3=Platanes sites. Lower panel: detail of the fault plane at Site 1. Note climber for scale.

2.1. Step 1: Sampling of Exhumed Limestone Scarps for REE Analysis

Once the appropriate section was selected (Site-1), a total of 54 limestone core-samples were extracted from the exhumed fault plane in an upscarp direction, every 30 cm. Each core-sample was 4 cm long and 2cm wide. Four samples were also extracted below the soil surface, down to depth of -0.7 m.

2.2. Step 2: Identification and Measurement of REE

This stage involved the following individual steps per limestone core-sample: removal of 2mm core coating, 2cm core slicing, manual core crashing down to less than sugar grain-size, digestion of limestone grains aided by a series of acids (chemical preparation stage), centrifugation of the solutions and finally measurement of the content of REE on each sample by Inductively Coupled Plasma Mass Spectrometry (ICP-MS) equipment.

The digestion of the limestone grains (chemical preparation stage) was achieved through the following individual steps:

a) Initial dissolution with HCl until dryness for carbonates removal;

b) Dilution with HNO_3;

c) Dissolution with a mixture of HF, HNO_3 HCl and digestion in microwave;

d) Addition of EDTA and second digestion in microwave;

e) Dryness and dilution with HNO_3.

Figure 2 - Sampling the lower 15 m of the Spili Fault at Site-1 for REE analysis (a) and the lower 9 m at Site-2 for cosmogenic dating (b) using a portable drill and rock-saw, respectively.

This analysis provided the number and size of the past earthquakes on each fault and took place at the Department of Environmental Engineering at the Technical University of Crete (laboratory: Hydrogeochemical engineering and remediation of soils).

2.3. Step 3: Cosmogenic Isotope Sampling

During this stage we extracted limestone-samples for [36]Cl cosmogenic dating of the earthquakes. S pecifically, we used an electric rock grinder to remove a 15cm wide and 3cm thick section of the e ntire exhumed limestone fault plane. This technique is used routinely for cosmogenic isotope datin g. During this stage we extracted a total of 208 samples for [36]Cl cosmogenic dating. Specifically, we extracted 106 samples from the Site 1, 82 samples from Site 2 and 20 samples from Site 3.

2.4. Step 4: Cosmogenic Dating of Prehistoric Earthquakes

The last step concerns the dating of each identified earthquake by determining the concentration of [36]Cl as a function of scarp height. [36]Cl is produced primarily through interaction of cosmic rays with Ca within the calcite ($CaCO_3$) of the limestone scarp. Because the production rate of [36]Cl and its distribution below the surface are known, the concentration of cosmogenic [36]Cl can be used to calculate how long a surface has been exposed to cosmic radiation. This analysis took place at the laboratory facilities of CNRS in France (Université Aix-Marseille III).

This analysis included the following individual steps: a) sample preparation for chemical Cl extraction, b) Accelerator Mass Spectrometry (AMS) measurements and [36]Cl concentration determination, c) analysis of host rock chemical composition, d) analysis of colluvial wedge chemical composition and e) determination of the density of the fault scarp rocks and colluvium (Schlagenhauf et al., 2010). The final measurements of [36]Cl concentrations provided the timing of each earthquake.

Some information about the rock sampling and crushing:

Sampling in all cases involved extraction of carbonate rock from near-vertical (~75-80°) fault-scarps. The equipment used included an electrical generator, portable drill or rock-saw, chisel, hammer and climbing equipment (Figures 2 & 3a). Following the extraction, we manually crushed (inside an agate mortar) the REE samples, after having removed the upper 2mm of the outer core coating (Figure 3b). Each core required about 40 minutes of manual crushing. We also crushed down to sugar-grain size using an electrical mill a total of 91 limestone slabs for [36]Cl analysis. Each slab required about 30 minutes. Subsequently we used a sheave to separate fractions of the crushed material (the [36]Cl content is measured on carbonate grain-sizes ranging from 250 to 500μm).
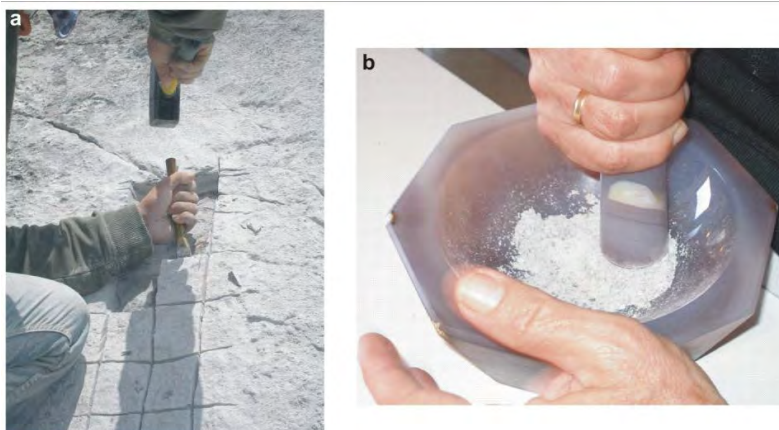

Figure 3 - (a) Sampling of the Spili Fault plane for cosmogenic dating; (b) Prior to the chemical treatment stage, carbonate cores extracted for REE analysis were manually crushed down to sugar grain size within an agate mortar.

3. Results

We successfully mapped the entire surface trace of the Spili Fault (~20 km) and identified three sections for sampling and subsequent analysis: the 'Spili' or Site-1, the 'Health Centre' or Site-2 and 'Platanes' or Site-3 (see yellow circles in Figure 1). Specifically, by combining REE measurements from the lower 15 m at Site-1 with ^{36}Cl measurements from the lower 9 m at Site-2 we recovered a minimum of seven paleoearthquakes that were accommodated by the Spili Fault and constrained the timing on the five most recent of these events.

The ^{36}Cl measurements from Site-1 are sparse and of low-concentration and thus difficult to interpret. The ^{36}Cl measurements from Site-3 are, up to date, inconclusive due to the high values of inherited Cl in the carbonates. For these reasons the above data are not included in the subsequent analysis and the timing of the identified earthquakes is based on measurements from Site 2.

3.1. Number, Size and Timing of Past Earthquake Activity on the Spili Fault

Seven paleoearthquakes have been identified to have ruptured the Spili Fault, the five most recent of which having occurred during the last ~16500 years. In the following sections, we discuss how individual earthquakes may be constrained on a fault scarp by combing the REE method with cosmogenic (^{36}Cl) dating.
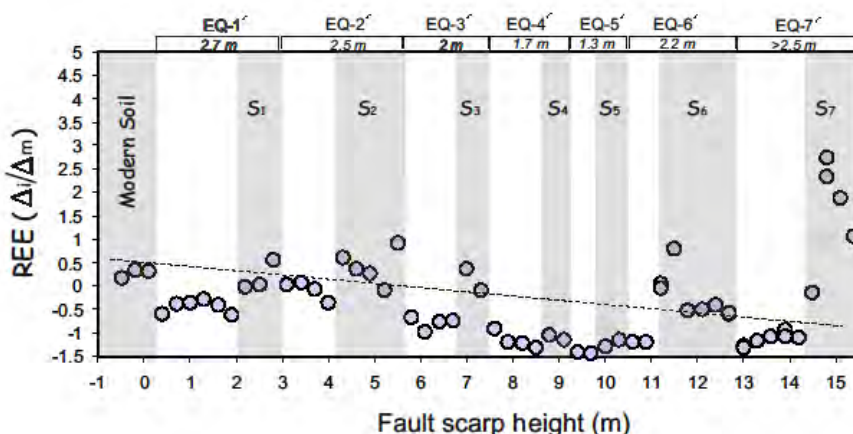

Figure 4 - (a) Plot showing the variability in the concentration of the REE as a function of sample position along the fault scarp. The Y-axis measures the difference Δi between a given concentration in core i (Ci) and the mean concentration (Cm) over the entire fault scarp collection (Δ*i*=C*i*-Cm), normalized to the mean absolute value of those differences (*Δm). Circles correspond to the average value of 14 different REE at each locality. Domains Si, which are shaded grey, indicate scarp sections enriched in REE. Dashed line indicates the decreasing trend (depletion) of the average *Δi/Δm* with increasing scarp height.

REE analysis: In order to constrain the number and size of the past earthquakes that ruptured the Spili Fault we measured the REE content at 54 upscarp localities at Site-1 (Figure 4). In Figure 4, where a concentration measure (*Δi/Δm*) is plotted as a function of fault scarp height, we explore the upscarp concentration evolution of the REE average. Specifically, the Y-axis in Figure 4 measures the difference (*Δi*) between a given concentration of an element (*i*) in core (*Ci*) and the mean concentration (*Cm*) of the same element over the entire fault scarp collection (Δ*i*=C*i*-*Cm*), normalized to the mean absolute value of those differences (*Δm)*. Data reveal a nearly linear decrease of the average REE concentration with increasing scarp height (dashed line in Figure 4).

The most striking feature illustrated in Figure 4 is that, superimposed on the overall depleting trend upscarp, there is a continuous and clear signal of fluctuations in the REE concentrations as a function of fault scarp height. In detail, there are domains in which the REE concentrations are locally increased. These domains, which are highlighted by grey shading in Figure 4, are always preceded or followed by scarp sections which are characterised by lower concentrations in REE. For example, the section of the fault scarp that is currently buried up to 0.5 m below the ground surface has, on average, 60% higher REE-Y concentration compared to the section of the scarp immediately above the ground surface (Figure 4). The 60% 'drop' in the concentration persists up to the height of about 2m, where another increase of ca. 75% in the REE concentration occurs (Figure 4). Overall, our data record a minimum of seven, such *'fluctuations'* in the concentration of REE on the lowest 15m of the Spili Fault plane (Figure 4).

According to the model presented in earlier studies (Manighetti et al., 2010; Mouslopoulou et al., 2011), each concentration fluctuation is associated with an earthquake event that instantly exhumed subaerially sections of the fault scarp with depleted and elevated REE concentrations. Thus, we have identified a minimum of seven such paleoearthquakes the size of which ranges from 1.3 to 2.7 m. For more information on the REE method, its uncertainties but also the actual REE measurements that derive from the 10 lower meters of the Site-1 on Spili Fault see Mouslopoulou et al. (2011).

Cosmogenic (^{36}cl) dating: We measured and modelled the content of *in situ cosmogenic ^{36}Cl* on 41 limestone samples extracted from the lower 9 m of the fault scarp at Site-2 (Figure 5). The total scarp height at this locality is ~12 m.

The modelling of the ^{36}Cl results has taken into account the dip of the fault at Site-2, the density and the dip of the alluvial fan, the dip of the older scarp section (above the sampling site) and the shading that may be induced locally by the surrounding topography (Schlagenhauf et al., 2010).

Results indicate that the lower section (~3.5 meters) of the fault scarp is much younger than the remaining scarp. Examination of the graph in Figure 5 reveals two sharp discontinuities at 1 and 3.5 meters along the height of the scarp. These discontinuities are interpreted to result from at least two large magnitude earthquake events. The timing of these earthquakes is modelled to be at 500 (-400, +200) and 600 (±300) years BP, respectively. Following, at about 6m upscarp, there is another discontinuity, dated at 7300 (-300, +400) years BP. The large time-lag between the second and third identified earthquakes on the Spili Fault is reflected in the increased content in ^{36}Cl at six meters compared to the content measured lower on the scarp (the upper section of the scarp has been exposed to cosmic ray radiation for longer time-periods than the lower section of the scarp). This is also evident in the field, when one compares the roughness of the fault plane at different localities upscarp. Following, the 4th and 5th recorded discontinuities (earthquakes) are identified at 7.2 m and 9 m upscarp and their timing is modelled at 16300 (-100, +500) and 16500 (-500, +700) years BP, respectively (Figure 5).

The slip-sizes of the five most recent earthquakes identified at Site-2 (starting from the most recent: 1m, 2.5m, 2.5m, 1.2m and 1.8) are overall comparable to those derived from Site-1 by the REE method (starting from the most recent: 2.7m, 2.5m, 2m, 1.7m and 1.3m). Lateral slip variability is commonly observed along faults, even over short lateral distances (Schlagenhauf et al., 2011). In our case the two sites are located ~2 km apart and the slip variability observed is not surprising (perhaps with the exception of the most recent event).

Despite the fact that there have been at least 60 historically recorded large magnitude (>M6) earthquakes during the period 900-100 years BP (Papadopoulos, 2011), with some of them affecting mainly the area around Rethymnon, it is not possible to safely correlate any of the individual historic earthquakes to the identified paleoearthquakes on the Spili Fault (the uncertainties are large and include several large magnitude earthquakes).
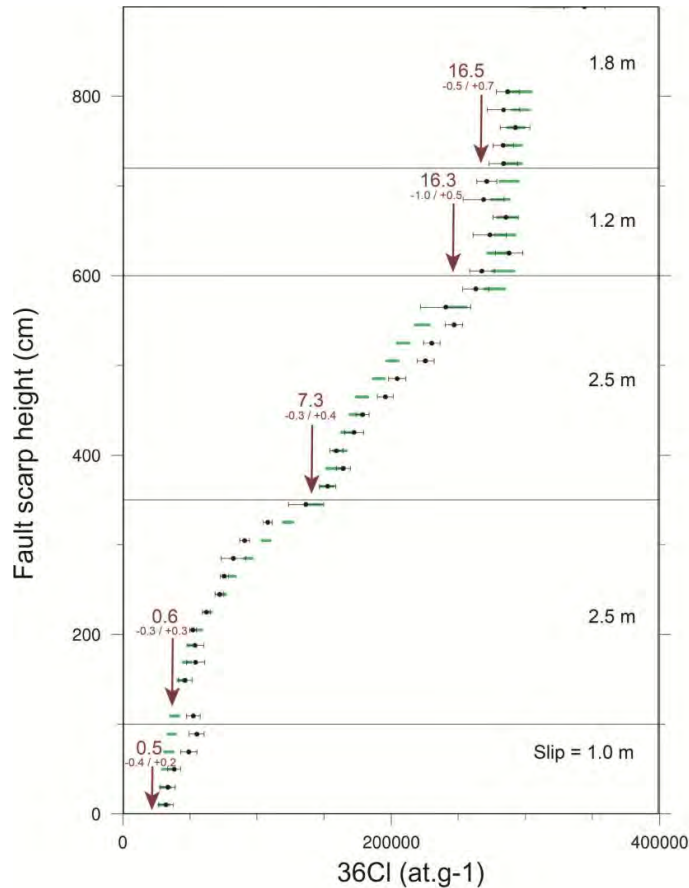
Figure 5 - Modelling (green bars) of the ³⁶**Cl concentrations (black circles) that derive from the lower 9m of the Spili Fault at Site-2. Each horizontal line represents a discontinuity that is interpreted to result from at least one paleoearthquake. The timing and slip-size of each earthquake is indicated on the graph.**

3.2. Earthquakes Parameters and Implications for Seismic Hazard

The Spili Fault is one of the most active faults on Crete. It has accrued 9 m of displacement over a period of 16000 years (Figure 6). Based on these measurements, the slip rate (SR) on the fault is ~ 0.6 mm/yr. Each identified earthquake on the Spili Fault produced co-seismic slip that ranged from 1 to ~2.7 m (Figure 6). Using the Wells and Coppersmiths equation M=6.69+0.74*log(MD), where MD is the Maximum Displacement per earthquake event, we derive earthquake magnitudes ranging from M 6.3-7.3.

Earthquakes of that magnitude may be highly damaging. Therefore it is important to discuss the frequency with which large magnitude earthquakes are accommodated by the Spili Fault. To achieve this, we introduce a term called 'earthquake recurrence interval'. The earthquake recurrence interval (RI) is the period of time between large magnitude events on an individual fault (McCalpin, 1996). The RI can be estimated using two different methods: 1) directly from the

earthquakes observed on the fault-scarp (observed RI) or 2) calculated from the mean single event displacement (SED) and the slip rate on the fault (estimated average RI). The methods are independent from one another and collectively provide a powerful means of estimating recurrence intervals and their variability.

Observed RI on the Spili Fault: Based on the timing of the five most recent earthquake events on the Spili Fault, that is 500, 600, 7300, 16300 and 16500 years BP and taking into account their respective uncertainties, we derive the following four RI's: 0-800, 6100-7400, 8500-9800 and 0-1000.

Therefore, based on these observed time intervals, the average observed RI on the Spili Fault over the last 16500 years is ~4200 years.
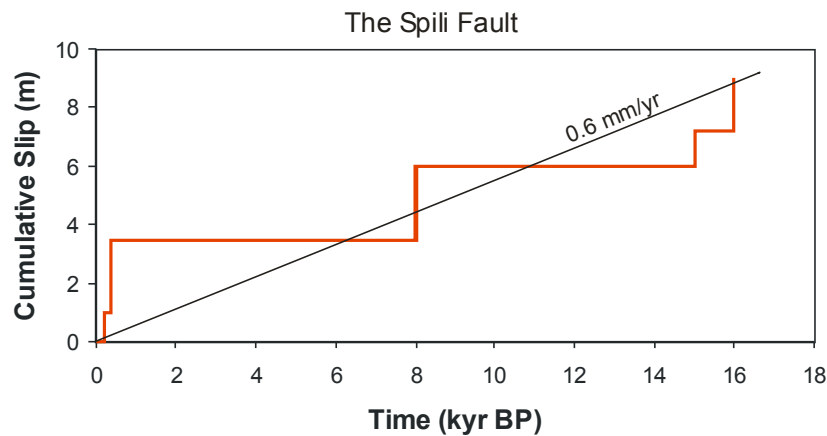

Figure 6 – Displacement versus time plot illustrating the accumulation of slip on the Spili Fault during the last 16.5 kyr. Each step corresponds to an earthquake event. The displacement rate on the fault averaged over the last 16.5 kyr is ca. 0.6 mm/yr.

Calculated RI on the Spili Fault: The value of "calculated average recurrence interval" is based on the cumulative displacement of a dated feature (fault-scarp in our case) that has been offset by multiple earthquakes. The slip per event (D) is typically estimated from the maximum or average slip documented during single earthquakes. The average D for the Spili Fault is 1.8m. Knowing that the slip rate (SR) on the fault is 0.6 mm/yr, we derive the calculated average recurrence interval based on the equation: $RI_{(calc)} = D/SR = 1800$ mm / 0.6 mm/yr = ca. 3000 years.

The above data suggest that the calculated (~3000 year) average recurrence interval on the Spili Fault is, within uncertainties, comparable to that observed (~4200 years) on the fault by dating individual earthquakes. This is encouraging because it may suggest that our sampling window (e.g. 16500) is large enough to overcome the short-term variability that often arises when we sample fault activity that is not representative of the long-term fault's behaviour (e.g. temporally clustered earthquake events). For example, the observed RI on the Spili Fault would have been much shorter had we only sampled the two most recent earthquakes on the fault. Nevertheless, as earthquakes on faults rarely occur periodically, the numbers associated with the earthquake recurrence intervals on a fault should be treated only as averages (Mouslopoulou et al., 2009).

4. Acknowledgments

5. References

Angelier J. 1979. Neotectonique de l'arc egeen, *Soc. Geol. Nord. Spec. Publ.,* 3, pp. 418.

Benedetti L., Finkel R., Papanastassiou D., King G., Armijo R., Ryerson F.J., Farber D. and Flerit, F. 2002. Post-glacial slip history of the Sparta fault (Greece) determined by [36]Cl cosmogenic dating: evidence for non-periodic earthquakes, *Geophys. Res. Lett.,* 29, 8701-8704.

Manighetti I., Boucher E., Chauvel A., Schlagenhauf A. and Benedetti L.2010. Rare earth elements record past earthquakes on exhumed limestone fault planes, *Terra Nova*, 22, 477-482.

McCalpin J.P. 1996. Paleoseismology: San Diego, California, Academic Press, 588.

Monaco C. and Tortorici L.2004. Faulting and effects of earthquakes on Minoan archaeological sites in Crete (Greece), *Tectonophysics*, 382, 103-116.

Mouslopoulou V., Walsh J.J. and Nicol, A. 2009. Fault displacement rates on a range of time-scales, *Earth Planet. Sci. Lett.*, 278, 186-197.

Mouslopoulou V., Moraetis D. and Fassoulas C. 2011. Identifying past earthquakes on carbonate faults: advances and limitations of the Rare Earth Element method based on analysis of the Spili Fault, Crete, Greece, *Earth Planet. Sci. Lett.*, 309, 45-55.

Nicol A., Walsh J.J., Mouslopoulou V and Villamor P.2009. Earthquake histories and Holocene acceleration of fault displacement rates, *Geology*, 37, 911–914.

Papadopoulos G. 2011. *A seismic history of Crete*, 0-416, Edition Oselotos, ISBN: 9789609499682

Schlagenhauf A., Gaudemer Y., Benedetti L., Manighetti I., Palumbo L., Schimmelpfennig I., Finkel R. and Pou K. 2010. Using in-situ Chlorine-36 cosmo-nuclide to recover past earthquake histories on limestone normal fault scarps: A reappraisal of methodology and interpretations, *Geophys. J. Intern.,* 182, 36–72.

Schlagenhauf A., Manighetti I., Benedetti L., Gaudemer Y., Finkel R., Malavieille J. and Pou K. 2011.Earthquake supercycles in central Italy, inferred from [36]Cl exposure dating, *Earth Planet. Sci. Lett.,* 307, 487–500.

Stein R.S., King G.C. and Rundle J.B. 1988. The growth of geological structures by repeated earth quakes: 2 Field examples of continental dip-slip faults, *J. Geophys. Res,* 93, 13319–13331.

Wells D.L. and Coppersmith K.J. 1994. New empirical relationships among magnitude, rupture length, rupture width, rupture area and surface displacement, *Bull. Seismol. Soc. Am.,* 8, 974-100.